Final Draft
of the original manuscript:

Ferreira, A.; Campanelli, L.; Suhuddin, U.; Alcantara, N.; dos Santos, J.:
Investigation of internal defects and premature fracture of dissimilar refill friction stir spot welds of AA5754 and AA6061.
In: The International Journal of Advanced Manufacturing Technology. Vol. 106 (2020) 3523 – 3531.
First published online by Springer: 06.01.2020

https://dx.doi.org/10.1007/s00170-019-04819-3

Investigation of internal defects and premature fracture of dissimilar refill friction stir spot welds of AA5754 and AA6061

Antonio Cappelletti Ferreira[1,2], Uceu Fuad Hasan Suhuddin[1], Leonardo Contri Campanelli[2], Nelson Guedes de Alcântara[2], Jorge Fernandez dos Santos[1]

[1] Helmholtz-Zentrum Geesthacht, Materials Mechanics, Solid-State Joining Processes, Institute of Materials Research, Max-Planck-Str. Geesthacht, Germany

[2] Materials Engineering Department, Federal University of São Carlos, R. Washington Luís Km 235—SP 310, Sao Carlos, Brazil

Abstract

The occurrence of internal defects in welded samples of AA5754-AA6061 produced by refill friction stir spot welding was investigated. A design of experiments using Box-Behnken method followed by a statistical examination using analysis of variance (ANOVA) and response surface modeling were utilized as analysis tools, which proved to be a reliable optimization methodology. This optimization successfully produced sound joints with high lap-shear strength. The statistical analysis showed a large influence of linear plunge depth, quadratic rotational speed, and two-way interaction of feeding rate and rotational speed on lap-shear strength of the welds. A quadratic hypersurface model for predicting weld performance was successfully generated. The subsequent investigation was performed by changing welding parameters, one factor at a time (OFAT), which confirmed the high dependence of lap-shear strength on rotational speed by producing an undesirable outlier. Metallographical analysis on the outlier sample pointed out the occurrence of voids and refilling defects, associated in large scale to low friction heat input. The outlier sample also produced a wing-shaped structure that possibly obstructed the flow of softened material toward void closure. The existence of those defects shows evidence of premature crack in the outlier sample. A subtle adjustment in rotational speed to1000 rpm proved to be sufficient to eliminate the defects and produce stronger welds. Although the problem of refilling defects could be solved, the mechanical properties in the weld were worsened compared to that of base material.

Introduction

Refill FSSW has been proven to be especially suitable to join aluminum in applications where dissimilar combinations of alloys are used. AA5754 and AA6061 are largely used in the form of sheets in car production, and a dissimilar contact between both alloys is fairly common in car assemblies. AA5754 is a work-hardening alloy commonly used for internal body panels and body structures, whereas AA6061 is an age-hardening alloy used in both internal and external body panels due to its better surface finishing after forming [1]. The sheets of car body panels and structure receive approximately 4.800 spot welds by resistance spot welding (RSW) [2], which represents high energy consumption and poor dendritic microstructure in the weld zone, leading to a high failure rate due to material fatigue. When applied to high–thermal conductivity aluminum alloys, resistance spot welding (RSW) produces large heat-affected zones (HAZ) and internal defects, such as solidification cracks and coarse dendritic structure. Refill FSSW, on the other hand, offers dimensionally reduced HAZ and a more refined microstructure, making it a potential candidate for replacing RSW.

Some works have recently been published in the field of friction stir spot welding (FSSW) of 5XXX and 6XXX series. By varying only the rotational speed (RS) process parameter, Patel et al. [3] successfully obtained defect-free dissimilar joints of AA5052 and AA6082 alloys and found that higher levels of RS

lead to better mechanical performance. In fact, RS has been shown to play a significant role on the performance of friction stir-based processes, as reported by Golezani et al. [4] on the primary friction stir welds of AA7010 alloy. The development by Saju et al. [5] of a new variant of FSSW for the dissimilar joining of AA5052 and AA6161 alloys confirms the current interest in this area. In this case, a pinless flat stir tool eliminated pinhole and hook formation, the defects inherent to FSSW. Concerning specifically the AA5754 and AA6061 alloys, Gerlich et al. [6] deeply studied the material flow, strain rates, and local melting slippage during FSSW.

Although some papers have been published on the welding of 5XXX and 6XXX series by FSSW, and only few on AA5754 and AA6061 alloys, there are no works about Refill FSSW on these alloys. Refill FSSW is a technique that makes use of a different tool assembly and parameters and therefore fundamentally differs from FSSW. In their review about friction stir-based processes for joining dissimilar metals, Chen et al. [7] mentioned that Refill FSSW has attracted more attention due to the absence of the keyhole typically left after the retraction of the welding tool. If well adjusted, Refill FSSW produces a stir zone at the same surface level of the base sheet, thus enhancing strength and fatigue life of the welded component. For that reason, in order to have the benefits of this superior welding technology, it is necessary to ensure that the processing window is suitable to produce welds with minimal defects.

Although Refill FSSW produces fewer defects compared to traditional welding methods, problems may still occur if a certain combination of factors enables the appearing of voids and discontinuities that can act as crack initiators and premature fracture. The strength of welds produced by Refill FSSW is strongly influenced by factors such as processing parameters, base materials, and sheet thickness. Usually, weld strength is maximized for a given pair of materials and sheet geometry by optimizing the process parameters. This work, therefore, aims to investigate the effect of welding parameters on the occurrence of defects in samples of AA5754 and AA6061 aluminum alloys and the metallurgical phenomena underlying such defects. Box-Behnken experimental design (BBD) combined with response surface methodology (RSM) was utilized as a tool to determine a model for weld lap-shear strength as function of welding parameters.

Materials and methods

Specimen preparation and testing

In this work, 1.2-mm-thick AA5754-H22 and AA6061-T6 were chosen as the base materials. All sheets were provided by The Welding Institute (TWI), UK, in the dimensions of 120 mm × 30 mm, as shown in Fig. 1. Before welding, the surfaces of all the sheets were cleaned with acetone to wipe off grease. Two sheets were welded in the center of the overlap area by Refill FSSW with 30 mm overlap being AA5754-H22 the upper sheet and AA6061-T6 the lower sheet. The lap-shear sample is designed to evaluate both tensile and shear joint strength, as the joint rotates during loading due to the low stiffness of the sheets [8].

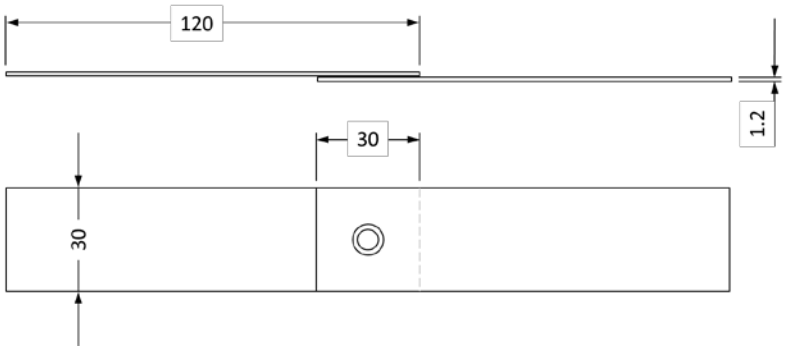

Fig. 1 - Technical drawing of friction spot-welded specimen. Units in millimeters

Refill FSSW was performed in a commercially RPS100® machine provided by Harms & Wende®. Outer diameters of the pin, the sleeve, and the clamping ring were 6, 9, and 18 mm, respectively. The sleeve had threads in the outer surface in order to provide a better mixing of the material. The process parameters rotational speed (RS), plunge depth (PD), and feeding rate (FR) were set in the built-in graphic user interface of the welding machine. Although many works studying dwell time (DT) instead of FR have been published [9,10,11], this work investigated FR as optimization parameter as it leads to shorter welding times and therefore is more production effective.

The measured welding force in the experiments was 12 kN. Overlap lap-shear samples were produced in a total welding time ranging from 1 to 2 s. Welds were tested for lap-shear strength (LSS) in a screw-driven Zwick/Roell® testing machine with a load capacity of 200 kN using a constant speed of 2 mm min−1 at room temperature. A concern of this study was to test the specimens in the same day they were prepared, because AA6061 is an age-hardening alloy. During tensile tests, the clamping area of the specimen was a 30 mm × 30 mm square as specified in ISO 14273 [12]. The separation gap between the clamps was 133.30 mm. The displacement rate was 2 mm.min−1.

Box-Behnken experimental design and optimization by RSM

Response surface methodology (RSM) is a powerful regression modeling technique that enables the development, improvement, and optimization of the process by offering the evaluation of the synergistic effects of a set of experimental factors on a response output. The methodology involves the input of data from an experimental design such as full-factorial, Taguchi, or Box-Behnken [13].

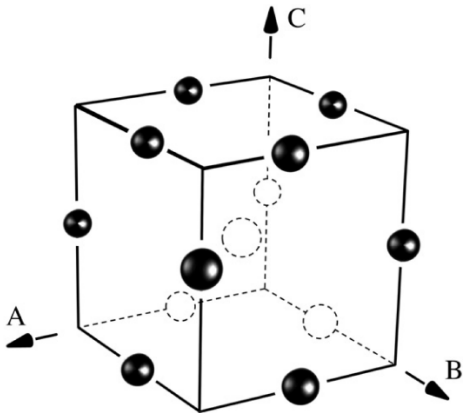

Fig. 2 - Scheme of the Box-Behnken design for three factors (from Vierneuse [14])

In the current work, a design of experiments (DoE) after BBD was preferred, given the requirement of analyzing quadratic relationships and the lowest possible number of necessary experiments. This design additionally shows no combination of extreme parameter settings due to a nonobservance of the design space edges, which might cause an unstable welding process (Fig. 2).

The process parameters RS (1000 rpm to 2000 rpm), PD (1.2 mm to 1.6 mm), and FR (3 mm s−1 to 4 mm s−1) were varied on three different levels according to Table 1. Prior to this study, preliminary tests were carried out to provide the range of parameters in which visually defect-free welds were produced. Through this, 13 combinations with widely varying lap-shear strength were achieved. For estimating the variance of the experiment within each treatment (sample), a triplicate of the central point is necessary. This leads to a number of 15 welds, which were organized and randomized by Minitab® according to Table 2. The specimens were welded according to the parameters and tested for maximum LSS.

Table 1 - Refill FSSW process parameters and levels

Symbol	Welding parameter	Unit	Level 1	Level 2	Level 3
			-1	0	1
RS	Rotational speed	rpm	1000	1500	2000
PD	Plunge depth	mm	1.2	1.4	1.6
FR	Retraction rate	$mm.s^{-1}$	3	3.5	4

Table 2 - Welding combination according to Box-Behnken design

Combination	Rotational speed (rpm)	Plunge depth (mm)	Feeding rate ($mm.s^{-1}$)
1	1000	1.4	3
2	1000	1.6	3.5
3	1500	1.4	3.5
4	1500	1.6	3.0
5	2000	1.2	3.5
6	1000	1.4	4.0
7	2000	1.4	4.0
8	2000	1.4	3.0
9	2000	1.6	3.5
10	1500	1.4	3.5
11	1500	1.6	4.0
12	1500	1.2	4.0
13	1500	1.4	3.5
14	1500	1.2	3.0
15	1000	1.2	3.5

A least-square algorithm built in Minitab® was used to find the coefficients that maximize the correlation between experimental data and the fitting curve. A quadratic model according to Eq. 1 was used.

$$y = \beta_0 + \sum_{i=1}^{k} \beta_i x_i + \sum_{i=1}^{k} \beta_{ii} x_i^2 + \sum_{i=1}^{k-1} \sum_{j=2}^{k} \beta_{ij} x_{ii} x_j + \epsilon \quad (1)$$

where y is the process response or output (dependent variable), k is the number of the patterns, i and j are the index numbers for pattern, β0 is the free or offset term called intercept term. x1. x2. ⋯. xk are the independent variables, βi are the coefficients of the first-order (linear) main effect, βii are the coefficients of the quadratic (squared) effect, βij are the coefficients of the interaction effect, and ε is the random error or admits discrepancies or uncertainties between predicted and measured values.

After the curve was fitted, it was possible to plot three-dimensional surfaces fixing one factor at the middle level. Parallel to this, an analysis of variance (ANOVA) was run to evaluate the fitting of the model, extracting information such as correlation, F test statistics, and p value. Significance levels (α) were set at 5% level using the p value test. ANOVA provides quantitative information about the fitting, whereas the surface enables us to see the contribution of factors by observing the declivity and twisting of the curve. The global fit of the model was determined by the coefficient of determination R2, and its significance was evaluated by a lack-of-fit F test.

After finding the surface region for which the LSS was the highest, a one-factor-at-a-time (OFAT) approach was used to extend the investigation. In this method, two parameters are fixed, and one is changed starting from a central point, which is chosen as the parameters that provide the best LSS results.

Results and discussion

Effect of process variables on LSS

The contribution of the welding process parameters on LSS has been statistically evaluated. A coefficient of determination (R2) of 0.856 indicated that the quadratic regression model was successfully fitted to experimental data. In order to evaluate how well the model fits to the experimental data, a lack-of-fit F test was performed. The F statistics is calculated using the equation below and compared with the tabulated F-distribution value for α = 0.05 and degrees of freedom 7 and 2, respectively, corresponding to the degrees of freedom of the lack-of-fit error and the pure error.

$$Adj\ MS_{lof} = \frac{MS_{lof}}{MS_{pe}} = 6.31 < F_{0.05,7,2} = 19.35$$

The lack-of-fit F test shows that the calculated F statistics is considerably lower than the tabulated F-distribution value. In addition, the calculated p value for lack of fit is significantly higher than the significance level, α = 0.05, which leads to the rejection of the hypothesis of an inadequacy of the model. The following hypersurface equation was generated from the least-square regression:

$$LSS = 9433 - 1.33 \cdot RS + 1297 \cdot PD - 2640 \cdot FR - 0.0017 \cdot RS^2 + 1.75 \cdot RS \cdot FR$$

The surface plots in Fig. 3, which display the effect and interaction of parameters on LSS, were generated using Python® programming language by fixing one parameter at mean position and using the remaining parameters as function domain. The three-dimension response surface curves and their corresponding contour plots show the interaction effects between each two parameters and have the function of indicating the optimum experimental conditions. The larger the surface gradient, the higher the influence of one parameter or a combination of parameters. In Fig. 3a, the steepest slope suggests that PD is the parameter with the largest linear contribution on LSS. The joint performance considerably increases with the increase of PD. Although the individual effect of FR on LSS is minimal, a significant interaction effect with RS is evidenced by the flexed shape of the surface in Fig. 3a and by

the deep drop on surface in Fig. 3b. Quadratic effect of RS is also noticeable by the parabolic shape of the surface along RS axis shown in Fig. 3b and Fig. 3c.

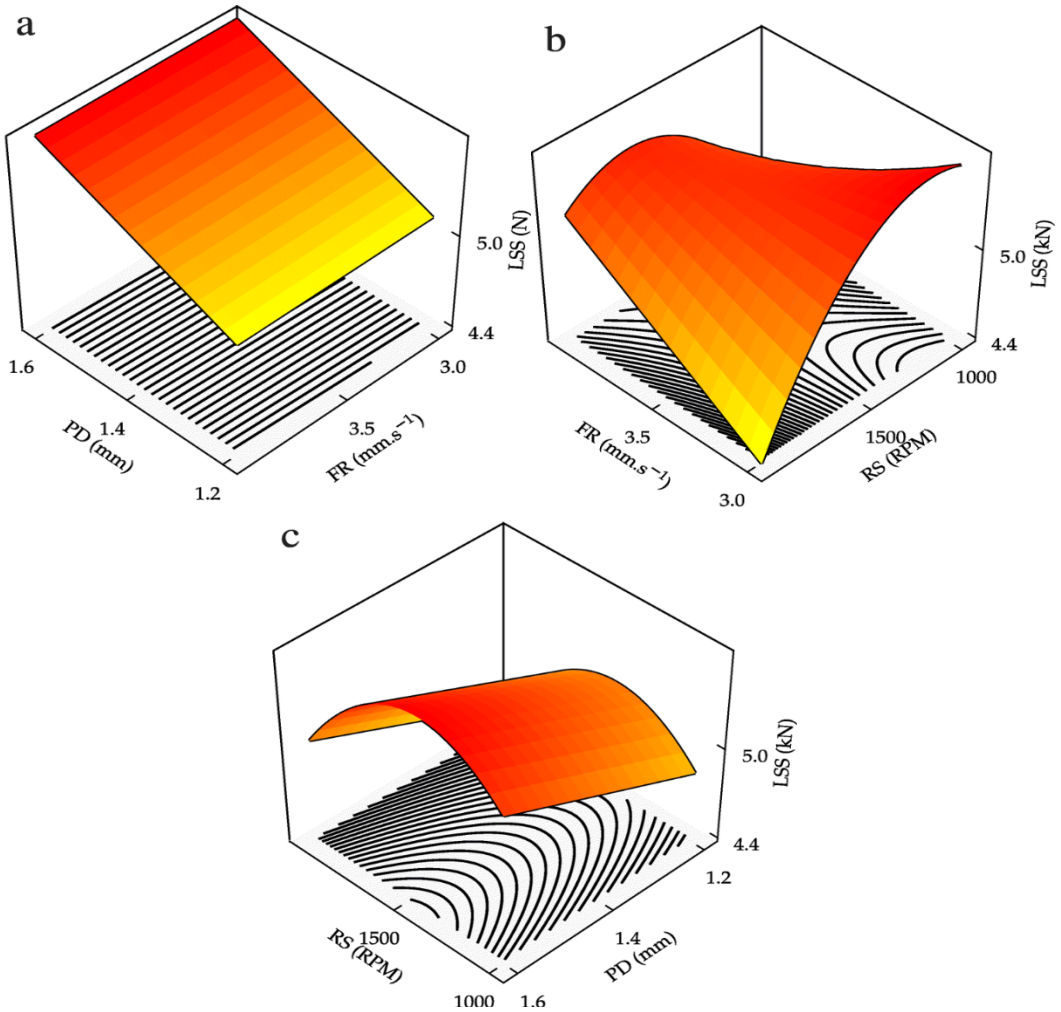

Fig. 3 - Response surface plot for LSS

A three-way ANOVA was carried out in order to examine main effects, interactions, and statistically significant differences between the means of the independent groups. The ANOVA results are shown in Table 3. Three main effects emerged, one on PD in the linear block of the model ($p = 0.005$), the square component RS × RS ($p = 0.003$), and the 2-way interaction component RS × FR ($p = 0.002$).

PD is the only factor in the linear block that influences the mechanical performance of the welds, with a contribution of 22%. The square component RS × RS and the 2-way interaction component RS × FR are also relevant for the model, with contributions of, respectively, 27% and 31.2%. Because RS and FR are relevant parameters in quadratic and 2-way components of the model, their contributions in the linear block were also accounted in this work, despite their insignificant influence in LSS.

Table 3 ANOVA (partial sum of squares) for response surface quadratic model

Source	SS	DF	MS	F-stat	P-value	Contrib. [%]
RS	131336	1	131336	3.3	0.101	5.4
PD	538623	1	538623	13.7	0.005	22.0
FR	471	1	471	0.0	0.915	0.0
RS × RS	660126	1	660126	16.8	0.003	27.0
RS × FR	765284	1	765284	19.5	0.002	31.2
Res. Error	353552	9	39284			14.4
Lack of Fit	338242	7	48320	6.31	0.144	13.8
Pure Error	15310	2	7655			0.6
Total	2449392	14				1.000

Optimization of parameters using OFAT

The model surface plots indicate that the most resistant welds are produced with parameters located around the red/orange areas of the surface plots. For this study, the central point with parameters RS = 1150, PD = 1.6, and FR = 3.0, located in the red region of the surface, was chosen.

In Fig. 4, OFAT results are shown in three-line scatter charts with standard deviation bars and a box-and-whisker plot of the means of OFAT results, which are useful to describe data distribution. From the box-and-whisker plot, values are narrowly distributed into an interval between 5650 and 5800 N. This chart also shows a sample that lies in an abnormal distance from the other values, i.e., an outlier, which fractured at 4373 N.

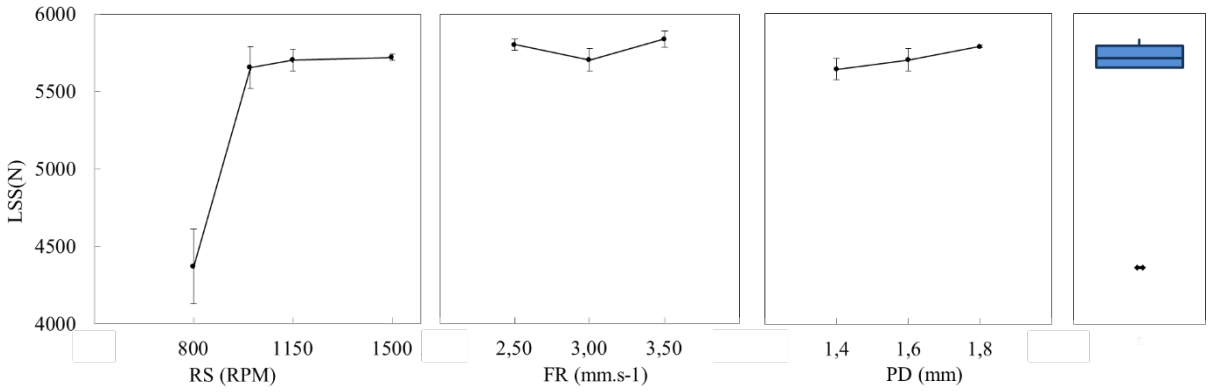

Fig. 4 - Effect of welding parameters on the LSS. (a) RS, (b) FR, (c) PD, and (d) Box-and-whisker plot of OFAT results means.

This outlier was identified as being the set of parameters RS = 800, PD = 1.6, and FR = 3.0. The relatively low RS was possibly responsible for the poor mechanical performance of this specific set of parameters. RS is directly correlated with frictional heat generated in the process, which in turn is responsible for material ductility during severe plastic deformation [15]. Although a higher RS would cause dissolution of precipitates and a higher amount of annealed material [16], an insufficient frictional heat can lead to internal cracks in weld cavity as well as lack of filling defects, which are even more detrimental to mechanical performance. To confirm the occurrence of such defects, a metallographic sample was obtained in the same weld conditions and observed under the microscope.

Cross section and defects

In Fig. 5, the weld zone cross-sectional micrograph of the outlier is shown. An incomplete refilling defect occurs near the joint upper surface. Void defects, which are located near the region known as “hook,” can also be observed. Hook is a typical feature for lap joints [9,10,11]. Additionally, the occurrence of regions of partially bonded material in the bonding ligament is observed. Both the incomplete refilling and void, indicated by the red circle, are located in the TMAZ/SZ interface, which is the region that undergoes high heat and plastic deformation. An early rupture during lap-shear testing due to the stress concentration effect around the defects is a probable cause of the lower mechanical performance of the outlier sample.

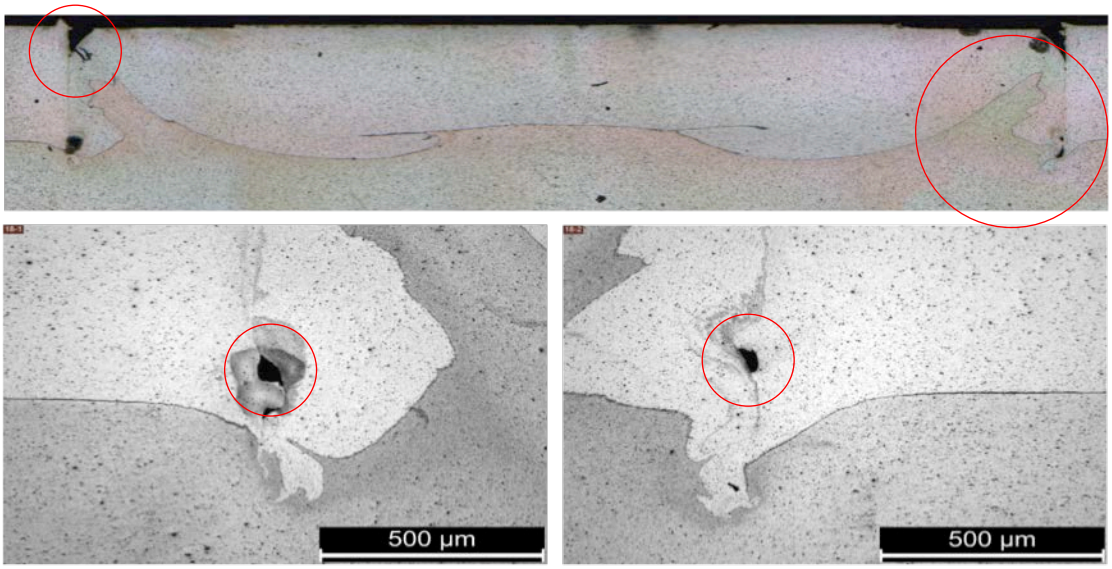

Fig. 5 - Cross section of outlier sample and hook zones. (a) Low-magnification overview, (b) left hook, (c) right hook

In Fig. 6, it can be observed that the weld presented a fracture mode referred as “pull-out” in previous works [9, 10]. This type of fracture normally occurs in high-quality joints when a circumferential crack nucleated in the tip of the hook propagates completely around the stir zone [17]. Nevertheless, the presence of large voids and refilling defects in the weld represents a much more critical stress concentrator than the hook, causing the fracture to propagate in a much faster rate compared to the one that could nucleate at the lower sheet. The result is that the SZ is completely pulled out the upper sheet but remain attached to the lower sheet.

The existence of such large defects can be explained by the lack of sufficient heat input, which results in low flowability of the softened material, a non-sufficient metallurgical bond and high residual stresses coming from the cooling of the material.

It can be seen from Fig. 5 that the lower sheet material (AA 6061-T6) produced, near the defects, a wing-shaped structure originated by the material flow from the pin pushing pressure at the welding final stage. Those wing-shaped structures may have hindered the flow of the upper sheet material (AA5754-H22) toward void closure inside the weld cavity by making the path of flow longer and more tortuous. The cause for the formation of this type of structure and void defects probably relies on many factors, such as process temperature and materials involved.

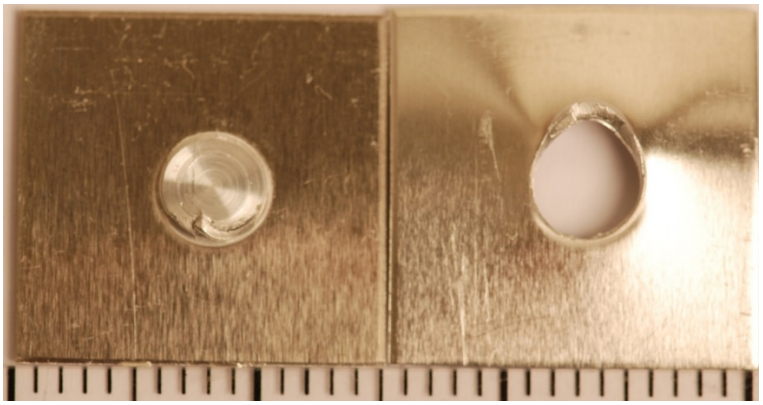

Fig. 6 - Macrography of fractured specimen of the outlier sample showing fracture mode

Previous works [15, 18] attributed the occurrence of voids to different circumstances that dictate material flow in the TMAZ/SZ. Xu et al. [19] also reported incomplete refilling and void defects in Refill FSSW of 2 mm 5083-O aluminum sheets. They attributed those defects to an insufficient flow of the SZ material at the refilling stage. Once the material does not reach a sufficiently high temperature due to lower frictional heat, its flowability is reduced resulting in inability to fill the corners of the welding cavity. Another cause of insufficient refilling proposed by Song et al. [20] and hold by Xu et al. [19] is the weak metallurgical bonding effect and heat residual stress after welding. The different temperature cycles between TMAZ and SZ materials lead to residual stresses in TMAZ/SZ interface, which may cause the defects. Song et al. [20] suggested that the interface could be torn if the residual stresses exceed the bonding strength. Material loss during welding procedure is also pointed as a factor that contributes to insufficient refilling.

Although those explanations are reasonable to explain the occurrence of weld defects, few have been done to testify the physical manifestation of such phenomena. Indirect methods like computational simulations and hardness testing might be useful tools to study the occurrence of residual heat stresses in TMAZ/SZ interface. Cao et al. [21] recently simulated material flow in Refill FSSW by developing a finite element model based on Johnson-Cook equation to describe the dependence of stress on temperature, strain, and strain rate. The simulation evidenced that high-temperature spots are found in the hook region, thus giving support arguments for the heat residual stresses.

The metallurgical bonding effect could also have been decreased due to the presence of a thin newly formed oxide layer at the surface of the hot softened material. The presence of aluminum oxide at the outer skin can elevate the surface tension of the material, thus inhibiting metal-to-metal bonding. At higher RS, the intermixing of softened material is more intense, making it more difficult for an oxide layer to form. Torkamany et al. [22] also reported internal defects in dissimilar AA5754 and steel produced by laser welding. Higher surface tensions in material/air interfaces were presented as a factor that prevented molten metal to fill completely the bottom of weld cavity. Similarly, in a softened state, Refill FSSW depends on the metallurgical bonding to form sound welds. In a softened state, with oxide-free surfaces exposed to air, an oxide layer may form and modify the flow behavior of the material.

Another factor not considered by the authors is a centrifugal effect, when considering a non-inertial reference frame, caused by the rotation of the pin when the material is being inserted back to the weld cavity. At higher RS, the material is more prone to overcome the radial forces such as surface tensions that occur at the interface between the material and the entrapped air. Lower RS cause more material to remain in the center rather than in the corners of the weld cavity. Therefore, a competition between centripetal forces and surface tension is likely to occur.

In Fig. 7, a cross section of a weld produced with slightly higher RS and no defects is shown. The weld was produced with the parameters RS = 1000, PD = 1.6, and FR = 3.0. The wing-shaped structure is not found, as in the previous weld, neither are the voids in the hook region and on the upper sheet surface. At higher RS, the material develops enough temperature and flowability to completely close the voids. As no critical defects are found, the weld strength of this sample was 5655 N. Micrographies taken from other welding conditions were omitted as they were nearly identical.

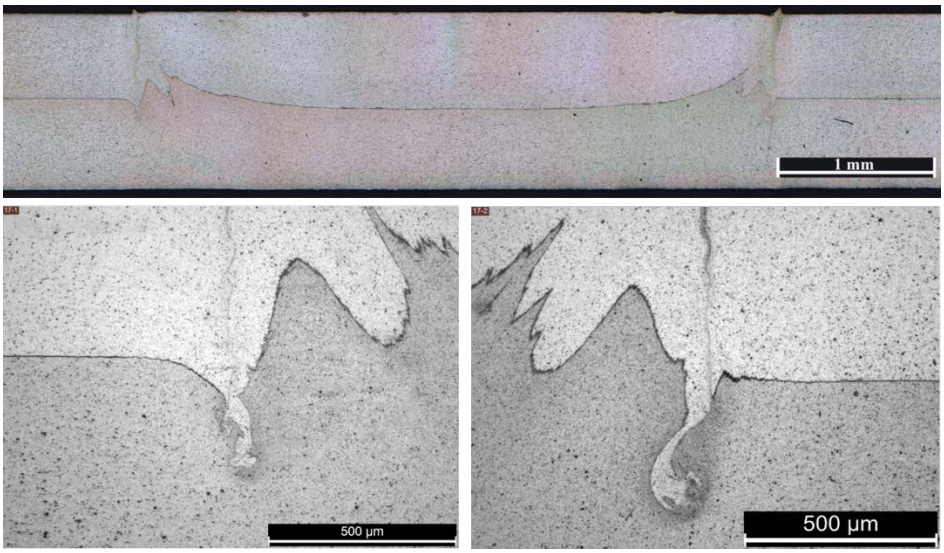

Fig. 7 - Cross section of sample produced without defects and its hook zones. a Low-magnification overview, b left hook, c right hook

The same condition was subjected to microhardness testing along its cross section in both sheets. The results are shown in Fig. 8. Hardness decreases in the weld and its surrounding area. The considerable softening of the material in the SZ and its surroundings in contrast to that in the BM can be explained by a significant coarsening and dissolution of precipitates in the lower sheet and decrease of dislocation density in the upper sheet, as previously reported by Zhang et al. [16] for AA5052 alloy. Although mechanical properties have deteriorated in the weld by this friction processing, this combination of parameters allowed the material to completely fill the weld cavity without leaving coarse defects, such as voids and lack of filling that occurred in the outlier sample of Fig. 5.

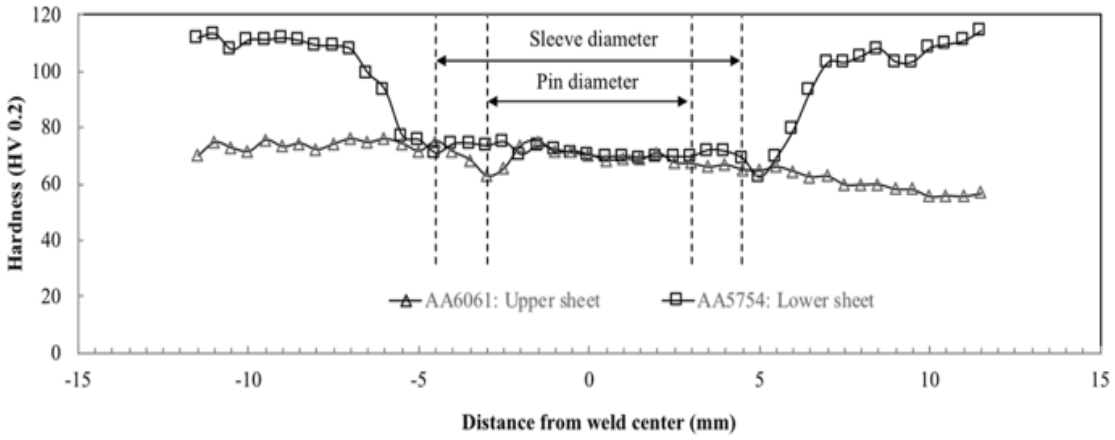

Fig. 8 Hardness profiles in both sheets of the weld. Parameters: RS = 1000; PD = 1.6; FR = 3.0

Conclusions

In this study, Refill FSSW was used to weld a dissimilar combination of 1.2-mm-thick AA5754 to AA6061. RSM and ANOVA were utilized as investigation tools for detecting statistical outliers due to inadequate welding parameters. ANOVA pointed linear PD, interactive FR-RS, and quadratic RS as the main factors to influence weld strength with contributions of, respectively, 22%, 27%, and 31.2% in lap-shear strength. OFAT experiments helped the identification of an outlier result for parameters RS = 800; PD = 1.6; and FR = 3.0. The lower mechanical performance of the outlier (4373 N) was attributed to the occurrence of refilling defects close to weld surface and near the hook identified in metallographic analysis. Low RS was pointed out as the main factor that influenced the formation of the defects. Defects were also linked to lack of material flowability, which is directly dependent on frictional heat. A wing-shaped feature formed by lower AA6061 sheet material was also pointed as a barrier for material flow, which might have hindered the closure of voids. Metallurgical bonding and material surface tension are also pointed as antagonist forces that influence the occurrence of internal defects. A slight increase of RS was sufficient to eliminate the occurrence of those internal defects and produce sound and strong welds.

References

1. Fridlyander IN, Sister VG, Grushko OE et al (2002) Aluminum alloys: promising materials in the automotive industry. Met Sci Heat Treat 44:365–370

2. de Alcântara NG, dos Santos JF (2015) FSpW valuation in the automotive industry

3. Patel VV, Sejani DJ, Patel NJ et al (2016) Effect of tool rotation speed on friction stir spot welded AA5052-H32 and AA6082-T6 dissimilar aluminum alloys. Metallogr Microstruct Anal 5:142–148

4. Golezani AS, Barenji RV, Heidarzadeh A, Pouraliakbar H (2015) Elucidating of tool rotational speed in friction stir welding of 7020-T6 aluminum alloy. Int J Adv Manuf Technol 81:1155–1164

5. Saju TP, Narayanan RG, Roy BS (2019) Effect of pinless tool shoulder diameter on dieless friction stir extrusion joining of AA 5052-H32 and AA 6061-T6 aluminum alloy sheets. J Mech Sci Technol 33:3981–3997

6. Gerlich A, Yamamoto M, North TH (2008) Local melting and tool slippage during friction stir spot welding of Al-alloys. J Mater Sci 43:2–11

7. Chen K, Liu X, Ni J (2019) A review of friction stir–based processes for joining dissimilar materials. Int J Adv Manuf Technol 1–23

8. Yang Y-P, Orth F, Peterson W, Gould J (2014) Accurate spot weld testing. Adv Mater Process 19

9. Plaine AH, Gonzalez AR, Suhuddin UFH et al (2015) The optimization of friction spot welding process parameters in AA6181-T4 and Ti6Al4V dissimilar joints. Mater Des 83:36–41

10. Campanelli LC, Suhuddin UFH, Dos Santos JF, Alcantara NG (2012) Preliminary investigation on friction spot welding of AZ31 magnesium alloy. In: Materials Science Forum. Trans Tech Publ, p 3016–3021

11. Prangnell PB, Bakavos D (2010) Novel approaches to friction spot welding thin aluminium automotive sheet. Materials Science Forum. Trans Tech Publ, In, pp 1237–1242

12. DIN E (2014) 14273. Specimen dimensions and procedure for tensile-shear testing resistance spot, seam and embossed projection welds. DIN, Ger Inst Stand

13. Khuri AI, Mukhopadhyay S (2010) Response surface methodology. Wiley Interdiscip Rev Comput Stat 2:128–149

14. Vierneusel B, Schneider T, Tremmel S et al (2013) Humidity resistant MoS2 coatings deposited by unbalanced magnetron sputtering. Surf Coat Technol 235:97–107

15. da Silva AAM, Meyer A, Dos Santos JF et al (2004) Mechanical and metallurgical properties of friction-welded TiC particulate reinforced Ti–6Al–4V. Compos Sci Technol 64:1495–1501

16. Zhang Z, Yang X, Zhang J et al (2011) Effect of welding parameters on microstructure and mechanical properties of friction stir spot welded 5052 aluminum alloy. Mater Des 32:4461–4470

17. Mazzaferro JAE, de Rosendo T, S, Mazzaferro CCP et al (2009) Preliminary study on the mechanical behavior of friction spot welds. Soldag Inspeção 14:238–247

18. Brzostek RC, Suhuddin U, dos Santos JF (2018) Fatigue assessment of refill friction stir spot weld in AA 2024-T3 similar joints. Fatigue Fract Eng Mater Struct 41:1208–1223

19. Xu Z, Li Z, Ji S, Zhang L (2017) Refill friction stir spot welding of 5083-O aluminum alloy. J Mater Sci Technol

20. Song Y, Yang X, Cui L et al (2014) Defect features and mechanical properties of friction stir lap welded dissimilar AA2024–AA7075 aluminum alloy sheets. Mater Des 55:9–18

21. Cao JY, Wang M, Kong L, Yin YH, Guo LJ (2017) Numerical modeling and experimental investigation of material flow in friction spot welding of Al 6061-T6. Int J Adv Manuf Technol 89:2129–2139.

22. Torkamany MJ, Tahamtan S, Sabbaghzadeh J (2010) Dissimilar welding of carbon steel to 5754 aluminum alloy by Nd: YAG pulsed laser. Mater Des 31:458–465